



# The fabrication of nanochain structure of gold nanoparticles and its application in ractopamine sensing

Jiahua Duan, Dawei He\*, Wenshuo Wang\*, Yongchuan Liu, Hongpeng Wu, Yongsheng Wang, Ming Fu, Shulei Li

Key Laboratory of Luminescence and Optical Information, Ministry of Education, Institute of Optoelectronic Technology, Beijing Jiaotong University, Beijing 100044, China

## ARTICLE INFO

### Article history:

Received 19 January 2013

Received in revised form

15 April 2013

Accepted 21 April 2013

Available online 9 May 2013

### Keywords:

Gold nanoparticles

Nanochain

Ractopamine

Melamine

Detection

## ABSTRACT

The illegal food additives including ractopamine and melamine throw a serious threat to human health. In this paper, the ractopamine and melamine were first used to form the nanochain structure of citrate-stabilized gold nanoparticles (AuNPs) with a convenient and inexpensive method. The fabricated nanochain structure consisting of several AuNPs was characterized by Scanning Electron Microscopy. A new longitudinal surface plasma resonance, which could be adjusted from visible to near infrared range, was observed in absorption spectra due to the aggregation of AuNPs. This could be well explained by Finite Different Time Domain algorithm theoretically. As confirmed by Fourier Transform Infrared Spectroscopy, the complex formed by hydrogen-bonding interaction between melamine and ractopamine could effectively promote the aggregation of AuNPs that was useful to develop the sensitivity and selectivity for the detection of ractopamine. Hence, the plasmonic coupling phenomenon of gold nanochain could be applied in bio-assay for ractopamine through the change of solution's color and optical absorption band with naked eye or absorption spectra. The linear range was broadened to ( $1.23 \times 10^{-7}$  M,  $1.11 \times 10^{-6}$  M) and the limit of detection was extended to  $4.10 \times 10^{-8}$  M ( $S/N=3$ ). More importantly, this time-saving method will be promising in rapid and selective detection of  $\beta$ -agonist for clinical applications.

Crown Copyright © 2013 Published by Elsevier B.V. All rights reserved.

## 1. Introduction

Metal nanoparticles, such as gold, silver, platinum, and palladium, have drawn great attention due to their unique optical and electronic properties in recent years. Among them, gold nanoparticles (AuNPs) were successfully applied in biosensors [1], electrochemical sensors [2], and SERS [3] which was ascribed to their great conductivity, electro-catalytic property and good biocompatibility. As well known, the AuNPs solution is wine red and shows a morphology dependent absorption peak at about 520 nm due to its surface plasma resonance (SPR) and resonance light scattering (RLS) [4]. It was found that a new plasma band (700–900 nm) corresponding to the longitudinal plasma module appeared after adding compounds to form the aggregation of gold nanoparticles just like the gold nanorods [5]. The impact factors for the surface plasmon resonance energy of gold nanoparticles included their sizes, morphologies, and the interactions among the aggregated particles [6,7]. The interaction existed between nanoparticles

could enhance linear and nonlinear optical properties which were applied in SERS, sensors, catalysis and so on [8–10].

In order to improve the properties and applications of gold nanoparticles, it is very important to develop great and convenient methods for constructing AuNPs into multi-dimensional structures such as nanochain (1D), nanobelt (2D) or nanocomet (3D) [11]. Among them, the nanochain structure is the fundamental blocks to build 2D or 3D structures. Furthermore, the nanochain structure shows promising application in imaging and diagnosis of cancer or other disease due to its optical resonance wavelength in the near-infrared region of the biological water window, where the depth of penetration is enhanced because of the highest tissue transmissivity [12]. Along with the imaging and diagnostic applications, the developed optical properties of nanochain including absorption in near-infrared range and low scattering ratio of incident light have been successfully applied in photothermal damage of cancerous cells [13]. As reported in other literatures, many conjugated complexes, which included some sulfur containing ligands [14,15], divalent DNA conjugates [16], and polymers [17], surfactants [18], some inorganic salts like sodium borohydride [19] or bottom-up techniques [20] were used to achieve the nanochain structure of AuNPs. But all these methods have disadvantages including expensive reagents, time-consuming,

\* Corresponding authors. Tel./fax: +86 10 51688018.

E-mail addresses: [dwhe@bjtu.edu.cn](mailto:dwhe@bjtu.edu.cn) (D. He), [wangwinsome@gmail.com](mailto:wangwinsome@gmail.com) (W. Wang).

unstable aggregated AuNPs and so on. Hence, it is significantly meaningful to develop a cheap and simple way to form AuNPs nanochain structure.

Beta-adrenergic agonists are phenylethanolamine compounds including different substituent groups on the aromatic rings or aliphatic amino groups. It has been illegally used as feed additives for economic benefits due to its growth promising and protein accretion increasing effects in livestock [21]. However, when livestock was fed with  $\beta$ -agonists, the residue would stay in meat and liver for a long time which threatened health of people including muscle tremor, nervousness and cardiovascular disease [22,23]. On the other hand, many athletes took  $\beta$ -agonists for their anabolic effects based on the increase of lean muscle mass. In order to guarantee the health of civilians and the fairness of sports competitive matches,  $\beta$ -agonists have been banned by many governments and International Olympic Committee [24]. Among the 12  $\beta$ -agonists, ractopamine (Rac) which was one of most widely used in food additives threw lots of threats to the health of people. The illegal application of Rac has caused a large amount of serious food safety problems in China and other countries. Due to its high nitrogen content (66% in mass), another illicit food additive called melamine also caused severe healthy problems including renal failure and even death of infants in China in 2008 [25,26]. Based on all these facts, many methods have been developed to selectively detect  $\beta$ -agonists and melamine, which included high performance liquid chromatography (HPLC) [27,28], gas chromatography with Mass Spectrum (MS) [29,30], surface enhanced Raman spectrometry [31,32], electrochemical methods [33,34], capillary electrophoresis [35,36] and so on. But all these approaches rely on expensive apparatus, time-consuming pre-concentration and purification process, making them difficult to be applied for the on-site and real time detection of Rac or melamine. Hence, it is very meaningful to develop a rapid, cheap and convenient method for highly selective detection for Rac or melamine on real time.

In this paper, the Rac or melamine or complex (M-Rac) was first used for the fabrication of AuNPs nanochain structures. The formed AuNPs nanochain was stable within a few days. Due to the aggregation of AuNPs, a new longitudinal surface plasma resonance, which could be tuned by the adding amount of Rac or melamine, was observed in absorption spectrum. In order to explain the experimental phenomenon, Finite Different Time Domain (FDTD) theoretical algorithm was carried out. In turn, the color change of AuNPs solution or the variation of absorption spectrum could be applied in the sensitive detection of Rac or melamine. More importantly, the M-Rac complex could effectively enhance the aggregation of AuNPs due to their hydrogen-bonding interactions. Hence, it was first found that the sensitivity and selectivity of assay for Rac could be significantly improved in the presence of appropriate melamine. Furthermore, this new method is cheap, time-saving and promising in developing area.

## 2. Material and methods

### 2.1. Chemicals and reagents

All chemicals used in this work were of analytical grade and used as received without further treatment. The solutions were prepared with double distilled water purified with the Millipore system. Ractopamine hydrochloride was obtained from Sigma (USA). Melamine was purchased from sinopharm Chemical Reagent Co., Ltd. (Shanghai, China). Sodium citrate was obtained from Beijing Chemical works (Beijing, China).

### 2.2. Instruments

The pictures of solution were taken by a Sony digital camera. Scanning electron microscopic (SEM) images of AuNPs were obtained by an S-4800 (Hitachi, Japan) at 15.0 kV. The optical absorption spectra were recorded by a UV-3101 scanning spectrophotometer (Shimadzu, Japan) at room temperature. The FT-IR spectra of melamine and M-Rac were recorded in NICOLET 750 infrared spectrometer (USA) at room temperature; the samples were treated in the form of pellets with KBr.

### 2.3. Preparation of citrate-stabilized AuNPs

Gold nanoparticles were fabricated by the reduction of  $\text{HAuCl}_4$  with trisodium citrate as reported in other literatures [37]. Briefly, 500  $\mu\text{L}$  of  $\text{HAuCl}_4$  (25.4 mM) was injected into 40 mL boiling distilled water under vigorous stirring. A total of 900  $\mu\text{L}$  of trisodium citrate (34 mM) was rapidly injected into the boiling solution under refluxing until a wine red solution was obtained. After the suspension was gradually cooled down to room temperature under stirring, it was stored in a refrigerator at 4  $^{\circ}\text{C}$  for further use. The fabricated colloid consisting of spherical AuNPs showed a mean diameter of 60 nm as confirmed by the SEM.

### 2.4. The fabrication of AuNPs nanochain structure

The Rac and melamine stock solutions were prepared by dissolving them into double distilled water. As well known, the melamine has a higher tendency to be absorbed on the AuNPs surface in the neutral condition. Hence, the pH value of 7.0 was chosen for all solutions here. The fabrication experiments were carried out as follows: firstly, the melamine or Rac solutions were individually injected into wine red gold nanoparticles to get their minimum required concentration for aggregated AuNPs. Secondly, Rac was added into AuNPs solution in the presence of melamine ( $9.09 \times 10^{-7}$  M) to get aggregated AuNPs structure which displayed blue color. Lastly, the fabricated AuNPs nanochain was characterized by SEM and absorption spectra.

### 2.5. Colorimetric detection of Rac

The detection procedure was performed as follows: first, 10  $\mu\text{L}$  of different concentrations of Rac was added into 1000  $\mu\text{L}$  prepared wine red AuNPs solution with shaking for 2 min to get a stable solution. Second, the obtained solution was transferred into a spectrophotometric cell to collect each absorption spectrum. Third, different concentrations of Rac were added into AuNPs solutions in the presence of  $9.09 \times 10^{-7}$  M melamine. Last, the absorption spectrum of mixed suspension containing appropriate melamine was collected as reported above for the sensitively quantitative detection of Rac.

## 3. Results and discussion

### 3.1. Characterization

The morphologies of the gold nanoparticles with or without M-Rac are shown in Fig. 1. The successful fabrication of mono-dispersion state AuNPs is confirmed by SEM. After adding M-Rac, the nanochain structure, which is composed of three gold nanoparticles just like the following theoretical simulation, is obviously observed from the inset figure. Hence, the Rac acts as an effective cross-linking agent for the fabrication of AuNPs nanochain in the presence of appropriate melamine which corresponds to a molecular linker.

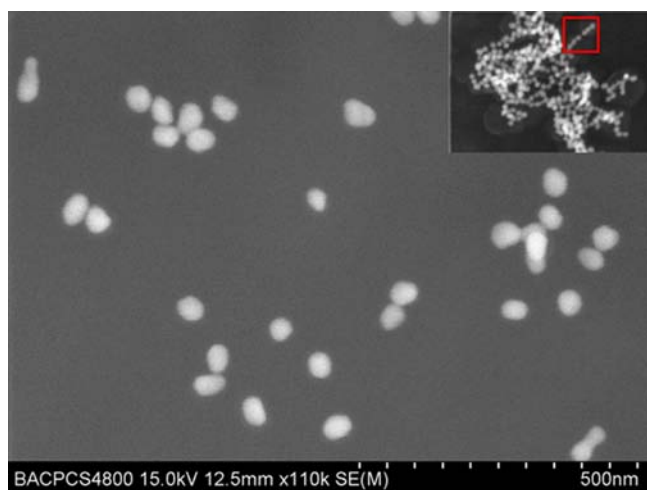


**Fig. 1.** SEM micrographs of fabricated AuNPs. Inlet: the nanochain structure of AuNPs with  $6.98 \times 10^{-7}$  M ractopamine in the presence of  $9.09 \times 10^{-7}$  M melamine.

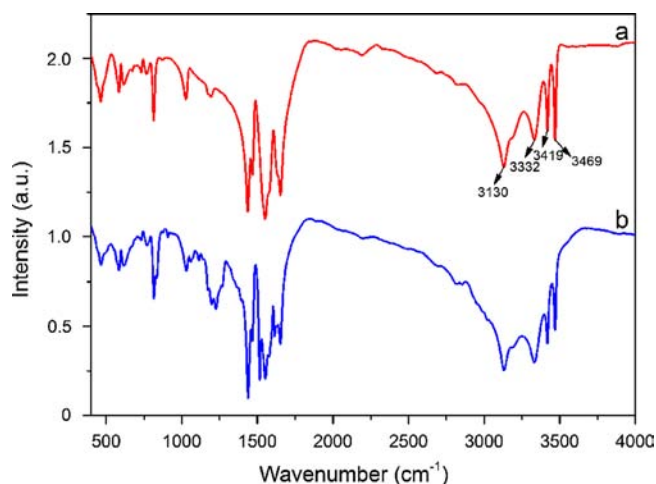


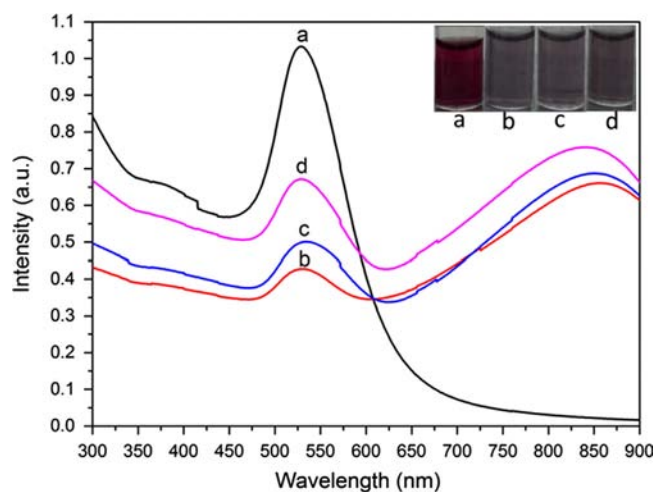
**Fig. 2.** FT-IR spectra of melamine (a) and the complex of melamine and ractopamine (b).

In order to confirm that the hydrogen-bonding interaction existed between Rac and melamine, the FT-IR spectra are performed. As well known, the higher wavenumbers range  $3000\text{--}3500\text{ cm}^{-1}$  corresponds to  $\text{--NH}$  vibration of melamine (Fig. 2a) [38]. After adding ractopamine, the mentioned bands have been significantly broadened (Fig. 2b), indicating the hydrogen-bonding interaction between  $\text{--OH}$  of Rac and  $\text{N--H}$  of melamine.

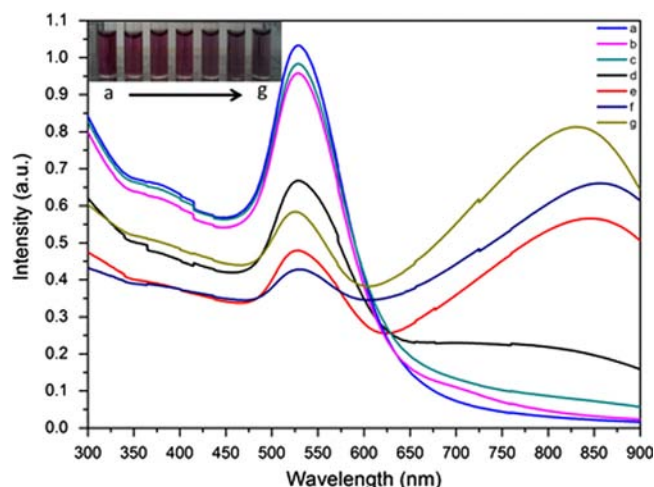
### 3.2. Formation of AuNPs nanochain structure

The extinction spectra and photos of dispersed AuNPs and nanochain structure are shown in Fig. 3. As shown, there is no new resonance band in the near-infrared range with the wine-red single AuNPs suspension. After adding melamine or Rac or M-Rac, the color of the suspension turns blue and a new absorption band of 830 nm is observed, indicating that the nanochain structure is constructed successfully. A few days later, the negligible change of spectra and color indicates that the prepared solution is very stable.

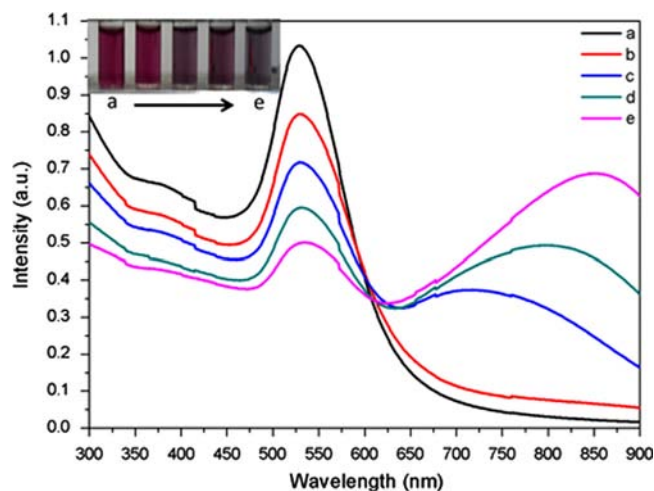
The SPR effect of gold nanoparticles has been reported thoroughly. When a single gold nanosphere is irradiated by incident electromagnetic wave, the electrical field will cause the relevant



**Fig. 3.** Absorption spectrum and photographs of AuNPs suspension with different additives: (a) pure AuNPs suspension, (b)  $1.11 \times 10^{-6}$  M melamine, (c)  $3.75 \times 10^{-6}$  M ractopamine, and (d)  $6.98 \times 10^{-7}$  M ractopamine in the presence of  $9.09 \times 10^{-7}$  M melamine.



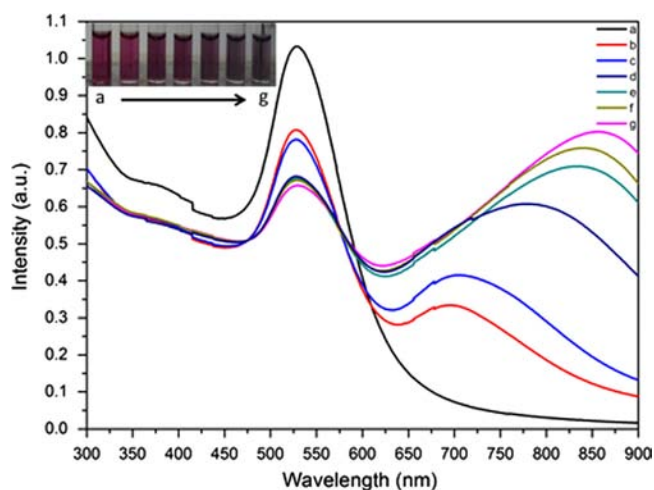
**Fig. 4.** The absorption spectrum and photos of different concentrations of melamine in AuNPs: (a) 0, (b)  $4.76 \times 10^{-7}$  M, (c)  $6.98 \times 10^{-7}$  M, (d)  $9.09 \times 10^{-7}$  M, (e)  $9.50 \times 10^{-7}$  M, (f)  $9.91 \times 10^{-7}$  M, and (g)  $1.11 \times 10^{-6}$  M.



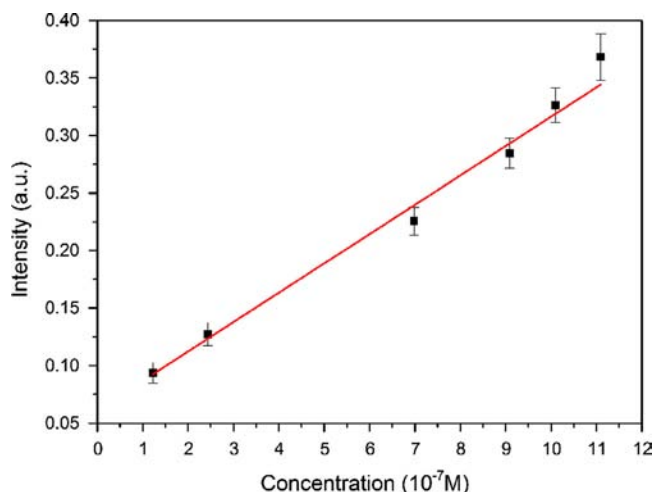
**Fig. 5.** The absorption spectrum and photos of different concentrations of ractopamine in AuNPs: (a) 0, (b)  $2.31 \times 10^{-6}$  M, (c)  $2.86 \times 10^{-6}$  M, (d)  $3.33 \times 10^{-6}$  M, and (e)  $3.75 \times 10^{-6}$  M.



resonance of AuNPs surface conduction electrons. The resonant wavelength for the dispersed state AuNPs is about 520–550 nm. After adding M-Rac, the extinction spectrum is represented by two bands: the dominant band (at longer wavelength) corresponding to the longitudinal resonance, and the intrinsic band (at shorter wavelength) corresponding to the transverse resonance. As shown





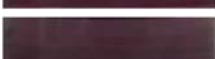

**Fig. 6.** The absorption spectrum and photos of different concentrations of ractopamine in the presence of  $9.09 \times 10^{-7}$  M melamine: (a) 0, (b)  $1.23 \times 10^{-7}$  M, (c)  $2.44 \times 10^{-7}$  M, (d)  $6.98 \times 10^{-7}$  M, (e)  $9.09 \times 10^{-7}$  M, (f)  $1.01 \times 10^{-6}$  M, and (g)  $1.11 \times 10^{-6}$  M.



**Fig. 7.** Linear relation between the intensity of AuNPs absorption band in the near infrared range and different concentrations of ractopamine in the presence of  $9.09 \times 10^{-7}$  M melamine.

**Table 1**

Colorimetric change of AuNPs solution corresponding to different concentrations of melamine and ractopamine (with or without melamine).

Color	Melamine	Ractopamine	Ractopamine with melamine
	$< 4.76 \times 10^{-7}$ M	$< 2.31 \times 10^{-6}$ M	$< 1.23 \times 10^{-7}$ M
	$4.76 \times 10^{-7}$ M– $9.09 \times 10^{-7}$ M	$2.31 \times 10^{-6}$ M– $2.86 \times 10^{-6}$ M	$1.23 \times 10^{-7}$ M– $6.98 \times 10^{-7}$ M
	$9.09 \times 10^{-7}$ M– $1.11 \times 10^{-6}$ M	$2.86 \times 10^{-6}$ M– $3.75 \times 10^{-6}$ M	$6.98 \times 10^{-7}$ M– $1.11 \times 10^{-6}$ M
	$> 1.11 \times 10^{-6}$ M	$> 3.75 \times 10^{-6}$ M	$> 1.11 \times 10^{-6}$ M

in Figs. 4–6, with addition of different concentrations of melamine or ractopamine or M-Rac, the absorption band of AuNPs solution can be tuned from 700 to 900 nm. The distance between two gold nanoparticles (3 nm), which is confirmed by SEM, is much shorter than the incident light wavelength. Hence, the optical properties of AuNPs nanochain structures depend on the individual particles and the near-field electro-dynamic interactions between them. As a single nanosphere, the extinction peak is at about 520 nm, which is ascribed to the isotropy SPR module due to its sphere morphology. Differently, the longitudinal resonance module becomes much longer than the transverse one when the nanochain structure of AuNPs is fabricated. This similar longitudinal resonance module to the gold nanorods demonstrates the successful fabrication of nanochain structure. This new resonance is observed in longer near-infrared range as a result of the delocalization existing between the conduction electrons of AuNPs and the conjugated compounds which is thanks to the direct adsorption of melamine or ractopamine. The delocalization of conduction electrons leads to quasi-conjugate structure which causes the decrease of resonated energy. The redshift and increasing peak intensity of the new longitudinal resonance, which relate to the increasing aspect ratio of nanochain structure, are observed with gradual addition of the above compounds.

On the other hand, with the addition of cross-link agents (melamine or ractopamine or M-Rac), the change of intrinsic resonant wavelength can be negligible, which may be ascribed to the almost unchanged transverse resonance module. But its intensity decreases during the gradual addition, due to the decreasing percentage of dispersed gold nanoparticles.

### 3.3. Sensitive detection of Rac

As shown in Figs. 4 and 5, it is worth noting that the minimum required concentration of melamine or Rac for the formation of nanochain structure is  $9.50 \times 10^{-7}$  M,  $2.86 \times 10^{-6}$  M, respectively. Hence, there is a higher tendency for melamine to be adsorbed on the surface of gold nanoparticles than Rac. In order to detect Rac sensitively and selectively, it is significant to add optimal concentration of melamine because only a balance state of melamine can effectively enhance the detection of Rac without adverse interference. As shown in Fig. 4, a dramatical change of UV–vis absorption spectrum is observed when the melamine concentration increases over  $9.09 \times 10^{-7}$  M. So,  $9.09 \times 10^{-7}$  M is intended to be the optimal concentration of melamine.

In order to verify the importance of melamine, the amount of Rac with or without melamine is detected. From Fig. 5, the limit of detection is high ( $2.86 \times 10^{-6}$  M) in the absence of melamine. After  $9.09 \times 10^{-7}$  M melamine is added, the limit of detection extends to  $4.10 \times 10^{-8}$  M (based on signal-to-noise ratio of 3) and linear range has been broadened to ( $1.23 \times 10^{-7}$  M,  $1.11 \times 10^{-6}$  M). The color of AuNPs suspension changes apparently from wine red, purple, to

**Table 2**Influence of potential interferents for detection of ractopamine ( $1 \text{ QUOTE} \times 10^{-6} \text{ M}$ ).

Coexisting substance	Concentration (M)	Relative error (%)
KCl	$1 \times 10^{-3}$	1.10
Na <sub>2</sub> SO <sub>4</sub>	$1 \times 10^{-3}$	1.15
NaCl	$1 \times 10^{-3}$	1.88
Alanine	$1 \times 10^{-3}$	2.87
Tryptophan	$1 \times 10^{-3}$	0.99
Glucose	$1 \times 10^{-3}$	4.56
Urea	$1 \times 10^{-3}$	0.42
Uric acid	$1 \times 10^{-4}$	2.36

**Table 3**

Determination and recovery test of ractopamine in pig urine sample.

Sample	Spiked (M)	Detected (M)	RSD <sup>a</sup> (%)	Recovery (%)	Average recovery (%)
A	$5.0 \times 10^{-7}$	$5.22 \times 10^{-7}$	1.83	104.4	
B	$7.5 \times 10^{-7}$	$7.66 \times 10^{-7}$	0.96	102.1	101.5
C	$1.0 \times 10^{-6}$	$9.80 \times 10^{-7}$	2.38	98	

<sup>a</sup> Three parallel samples are determined.

finally blue, which is ascribed to the aggregation of gold nanoparticles. As illustrated in Fig. 6, significant changes of absorption spectrum can be categorized as follows: (a) gradual decrease in SPR band at about 520 nm; (b) gradual increase and redshift of SPR band in the range of 700–900 nm. Based on these phenomena, the intensity of the new SPR band is used to quantify the concentration of ractopamine. A typical linear relation ( $R=0.9883$ ) between the band intensity in near-infrared range and the ractopamine concentration is represented in Fig. 7, which is very meaningful for the ractopamine's quantitative sensing. Based on the colorimetric change, the detection range of melamine and ractopamine (with or without melamine) is listed in Table 1, which is very useful in qualitative detection of melamine and ractopamine for the other tester. Through this method, it only costs a few minutes quantitatively or qualitatively to detect ractopamine with absorption spectrum or naked eye.

### 3.4. Effect of interferents

Some common potentially interfering substances are studied to testify the selectivity of this proposed assay method for ractopamine. The interference tests were performed under the optimized conditions, and the interferents were added individually. As shown in

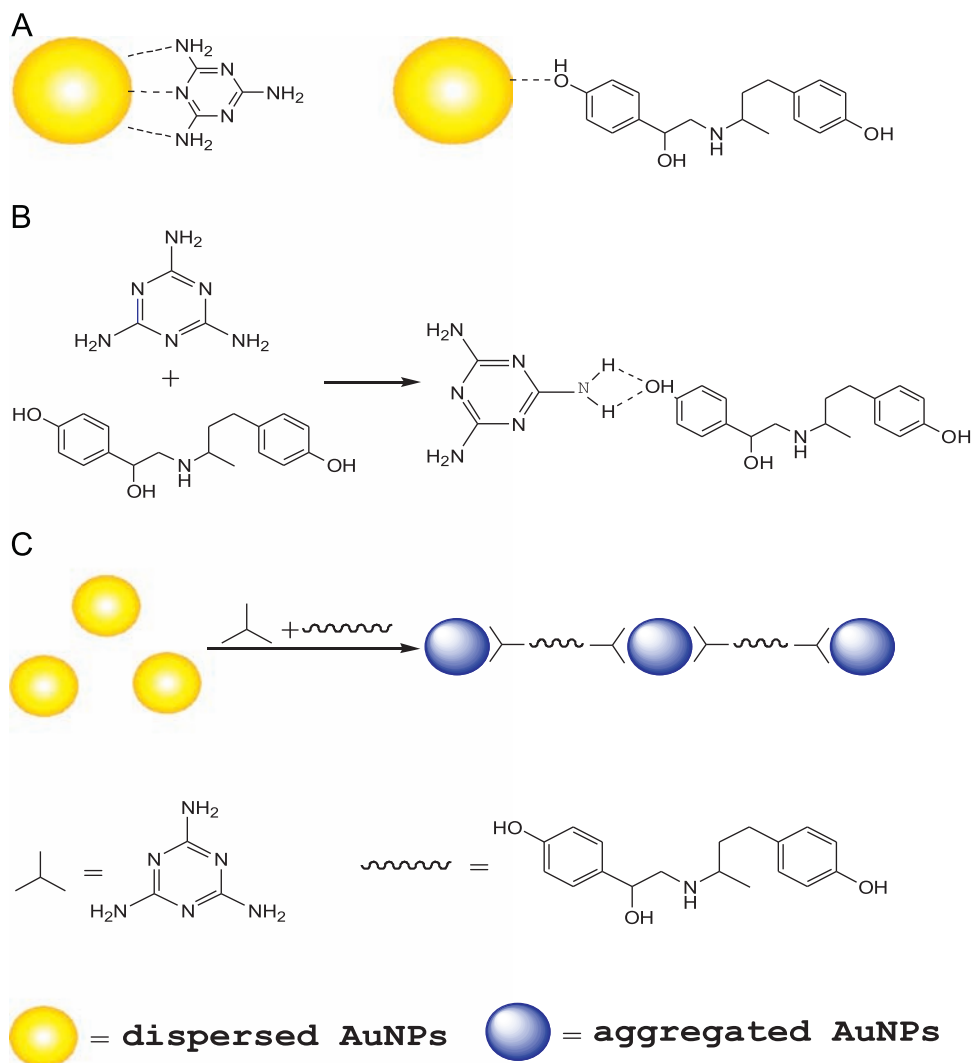


**Fig. 8.** Schematic picture of possible principle for the colorimetric detection of ractopamine: the interaction existing between AuNPs and melamine or ractopamine (A), the hydrogen-bonding interaction between melamine and ractopamine (B), and the formation of nanochain structure of AuNPs (C).

Table 2, no influence on the determination of  $1 \times 10^{-6}$  M ractopamine was found after the addition of the 1000-fold concentration of KCl,  $\text{Na}_2\text{SO}_4$ , NaCl, alanine, tryptophan, glucose, urea and 100-fold concentration of uric acid when the relative error was below 5%. These results show good selectivity of the proposed method.

### 3.5. Real samples analysis

This analytical method was used to detect trace amounts of ractopamine under optimized conditions in pig's urine which has been diluted 200 times with distilled water. No ractopamine was detected in the original pig's urine sample, so it was spiked with appropriate amount of ractopamine. The results and recoveries of known amounts of ractopamine added to the serum sample are given in Table 3. The presented results are satisfactory, showing that the proposed method can be successfully applied in practical determination of ractopamine concentration in urine samples.

### 3.6. Mechanism of colorimetric sensing

The solutions of single AuNPs are wine red due to its surface plasma resonance. It is found that many substances include electron-rich ligands which can be absorbed on the surface of AuNPs. As reported before [38], the melamine containing multiple electron-rich binding sites (three exocyclic amino groups and three nitrogen atoms on the hybrid aromatic rings) can be strongly absorbed on the surface of AuNPs. Hence, the aggregation of AuNPs will be fabricated by addition of melamine acting as a cross-linked agent. Another ractopamine  $\beta$ -agonist can also cause the aggregation of AuNPs because of its electron-rich phenolic groups. Furthermore, positively charged melamine or Rac can be absorbed on the surface of negatively charged AuNPs through electrostatic attractions as shown in Fig. 8A. As discussed above, there is a higher tendency for melamine to be absorbed on the surface of AuNPs than ractopamine.

Meanwhile, the hydrogen-bonding interaction between ractopamine and melamine as confirmed by FT-IR will form a supermolecule as shown in Fig. 8B. Hence, by adding appropriate melamine, the fabrication of AuNPs aggregation and the selectivity of ractopamine detection can be effectively enhanced as seen in Fig. 8C.

### 3.7. Theoretical explanation

The FDTD method is primitively used to calculate the optical properties of fabricated AuNPs nanochain structure. The final extinction spectrum is obtained by addition of absorption and scattering intensity. In order to achieve more accurate simulation, the size of gold nanoparticles is set as 60 nm and the distance between two nanospheres is determined as 3 nm just like the experimental condition. As shown in Fig. 9A and B, the calculated extinction spectrum displays different properties when the external applied electric field direction is parallel or perpendicular to the nanochain arrangement. In parallel circumstance, the resonance wavelength of nanochain structure shifts to about 700 nm in near-infrared range which is longer than the origin wavelength at 530 nm of dispersed nanoparticles according to the experimental condition. However, the change of long resonance wavelength can be relatively negligible in the perpendicular condition, indicating that the new longitudinal mode displays optical extinction only in parallel circumstance. This phenomenon may be ascribed to moving confinement effect of electrons in the perpendicular condition which needs more research. Opposite to the perpendicular condition, the scattering factor is larger than the absorption one in the parallel circumstance. As well known, the scattering factor is similarly larger than absorption with bigger

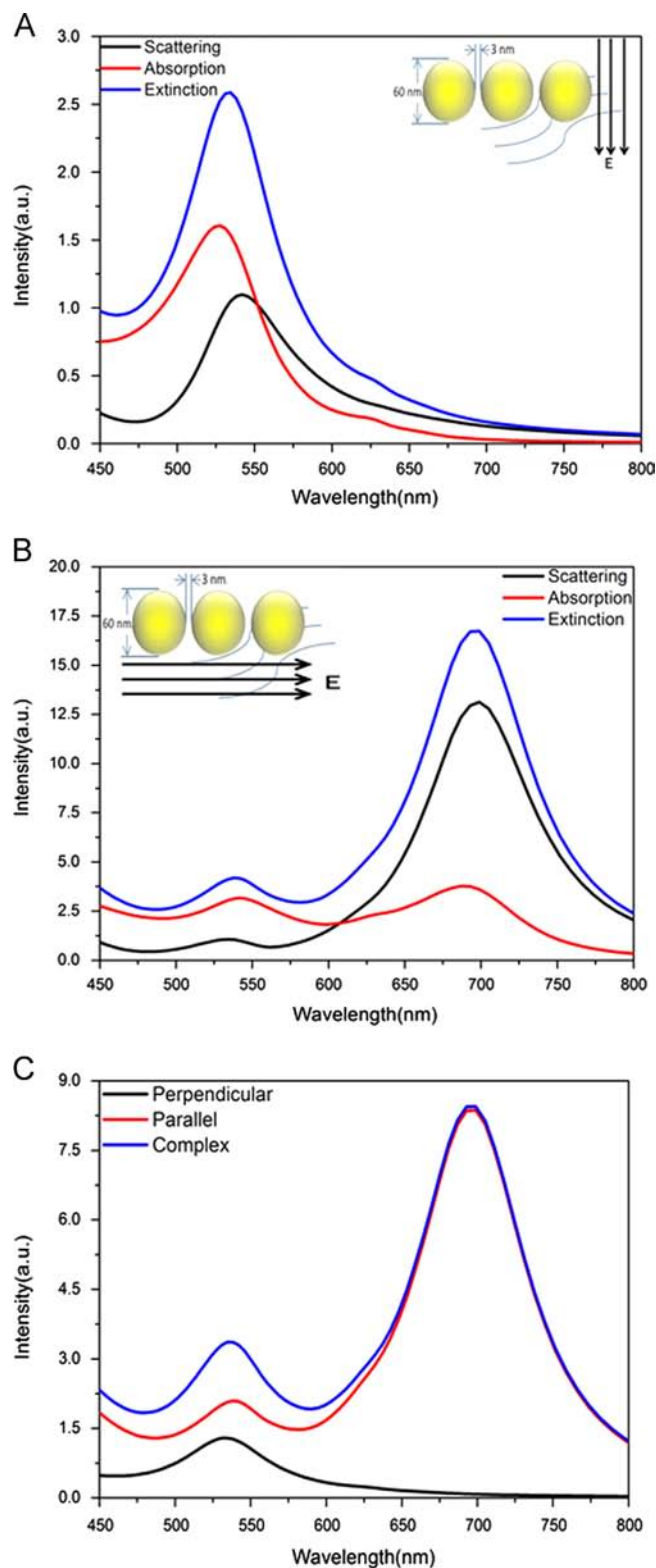


Fig. 9. FDTD calculated extinction spectrum of AuNPs nanochain structure in parallel (A), perpendicular (B), and ultimate (C) conditions. The size of gold nanoparticles is set as 60 nm and the distance between two nanospheres is determined as 3 nm.

size gold nanoparticles. The resemblance of the above results demonstrates the virgate geometrical configuration of AuNPs nanochain structure. Given that the incident natural light can be handled by the orthogonal decomposition method, the ultimate

calculated spectrogram (Fig. 9C) is constituted by equivalent parallel and perpendicular conditions, which fits well with the experimental data above. The consistency existing between theoretical simulation and experimental spectrum further indicates that the nanochain structure of gold nanoparticles is produced successfully.

#### 4. Conclusions

In this paper, a novel, convenient, cheap method for the fabrication of AuNPs nanochain structure was proposed. The melamine and Rac were first applied for the self-assembly of gold nanoparticles into nanochain structure. The produced AuNPs nanochain suspension was stable within a few days and the new longitudinal SPR band in the near-infrared range could be adjusted from visible to near-infrared range. The morphologies and size of AuNPs were characterized by SEM. Meanwhile, the strong hydrogen-bonding existing between melamine and ractopamine was verified by FT-IR. The change of absorption spectrum and color could be theoretically explained by the FDTD method. Interestingly, the complex of Rac and appropriate melamine was first found to effectively enhance the aggregation of AuNPs. So the sensitivity and selectivity for detection of Rac were developed in the presence of  $9.09 \times 10^{-7}$  M melamine. The limit of detection was extended to  $4.10 \times 10^{-8}$  M ( $S/N=3$ ) and the linear range was broadened to ( $1.23 \times 10^{-7}$  M  $1.11 \times 10^{-6}$  M). Due to the good sensitivity and selectivity, this time-saving method is a promising tool for determination of Rac in pig's urine samples.

#### Acknowledgment

The authors gratefully acknowledge the financial support from the National Basic Research Program 973: 2011CB932700, 2011CB932703, National Outstanding Youth Science Foundation under Contract no. 60825407, and National Natural Science Fund Project under Contract no. 61077044, 60877025, 91123025, Beijing Natural Science Fund Project under Contract no. 4132031, and the Fundamental Research Funds for the Central Universities of Beijing Jiaotong University under Contract no. 2012YJS124, 2013JBM097.

#### References

- [1] X. Wang, Y. Xu, X. Xu, K. Hu, M. Xiang, L. Li, F. Liu, N. Li, *Talanta* 82 (2010) 693–697.

- [2] B.K. Jena, C. Retna Raj, *Talanta* 76 (2008) 161–165.
- [3] X. Liu, L. Zhao, H. Shen, H. Xu, L. Lu, *Talanta* 83 (2011) 1023–1029.
- [4] H. Li, J. Guo, H. Ping, L. Liu, M. Zhang, F. Guan, C. Sun, Q. Zhang, *Talanta* 87 (2011) 93–99.
- [5] Y.Y. Yu, S.S. Chang, C.L. Lee, C.R.C. Wang, *J. Phys. Chem. B* 101 (1997) 6661–6664.
- [6] S. Lin, M. Li, E. Dujardin, C. Girard, S. Mann, *Adv. Mater.* 17 (2005) 2553–2559.
- [7] M.A. El-Sayed, *Acc. Chem. Res.* 34 (2001) 257–264.
- [8] S.M. Adams, S. Campione, J.D. Caldwell, F.J. Bezares, J.C. Culbertson, F. Capolino, R. Ragan, *Small* 8 (2012) 2239–2249.
- [9] J.J. Storhoff, A.A. Lazarides, R.C. Mucic, C.A. Mirkin, R.L. Letsinger, G.C. Schatz, *J. Am. Chem. Soc.* 122 (2000) 4640–4650.
- [10] L. Lu, G. Sun, H. Zhang, H. Wang, S. Xi, J. Hu, Z. Tian, R. Chen, *J. Mater. Chem.* 14 (2004) 1005–1009.
- [11] P. Wang, Q. Yu, Y. Long, S. Hu, J. Zhuang, X. Wang, *Nano Res.* 5 (2012) 283–291.
- [12] R. Weissleder, *Nat. Biotechnol.* 19 (2001) 316–317.
- [13] C. Loo, A. Lowery, N. Halas, J. West, R. Drezek, *Nano Lett.* 5 (2005) 709–711.
- [14] L.A. Porter Jr., D. Ji, S.L. Westcott, M. Graupe, R.S. Czernuszewicz, N.J. Halas, T. R. Lee, *Langmuir* 14 (1998) 7378–7386.
- [15] A. Manna, P.L. Chen, H. Akiyama, T.X. Wei, K. Tamada, W. Knoll, *Chem. Mater.* 15 (2003) 20–28.
- [16] Y. Ohya, N. Miyoshi, M. Hashizume, T. Tamaki, T. Uehara, S. Shingubara, A. Kuzuya, *Small* 8 (2012) 2335–2340.
- [17] R. Sardar, J.S. Shumaker-Parry, *Nano Lett.* 8 (2008) 731–736.
- [18] J. Carballido-Landeira, S. Goy-López, A.P. Muñozuri, P. Taboada, V. Mosquera, *ChemPhysChem* 13 (2012) 1347–1353.
- [19] Z. Zhang, Y. Wu, *Langmuir* 27 (2011) 9834–9842.
- [20] S. Gwo, M.H. Lin, C.L. He, H.Y. Chen, T. Teranishi, *Langmuir* 28 (2012) 8902–8908.
- [21] G. Brambilla, T. Cenci, F. Franconi, R. Galarini, A. Macri, F. Rondoni, M. Strozzi, A. Loizzo, *Toxicol. Lett.* 114 (2000) 47–53.
- [22] G. Mazzanti, C. Daniele, G. Boatto, G. Manca, G. Brambilla, A. Loizzo, *Toxicology* 187 (2003) 91–99.
- [23] L. Salleras, A. Dominguez, E. Mata, J.L. Taberner, I. Moro, P. Salvà, *Public Health Rep.* 110 (1995) 338.
- [24] A.A.M. Stolker, U.A.T. Brinkman, *J. Chromatogr. A* 1067 (2005) 15–53.
- [25] V. Bhalla, P.C. Grimm, G.M. Chertow, A.C. Pao, *Kidney Int.* 75 (2009) 774–779.
- [26] H. Xin, R. Stone, *Science* 322 (2008) 1310–1311.
- [27] M. Rambla-Alegre, J. Peris-Vicente, S. Marco-Peiró, B. Beltrán-Martinavarro, J. Esteve-Romero, *Talanta* 81 (2010) 894–900.
- [28] S. Wang, L. Liu, G. Fang, C. Zhang, J. He, *J. Sep. Sci.* 32 (2009) 1333–1339.
- [29] P. Lutter, M.C. Savoy-Perroud, E. Campos-Gimenez, L. Meyer, T. Goldmann, M. C. Bertholet, P. Mottier, A. Desmarchelier, F. Monard, C. Perrin, *Food Control* 22 (2011) 903–913.
- [30] L. He, Y. Su, Z. Zeng, Y. Liu, X. Huang, *Anim. Feed Sci. Technol.* 132 (2007) 316–323.
- [31] H. Huang, C. Shende, A. Sengupta, F. Inscore, C. Brouillette, W. Smith, S. Farquharson, *J. Raman Spectrosc.* 43 (2012) 701–705.
- [32] F. Zhai, Y. Huang, C. Li, X. Wang, K. Lai, *J. Agric. Food Chem.* 59 (2011) 10023–10027.
- [33] Q. Cao, H. Zhao, L. Zeng, J. Wang, R. Wang, X. Qiu, Y. He, *Talanta* 80 (2009) 484–488.
- [34] C. Wu, D. Sun, Q. Li, K. Wu, *Sensor. Actuat. B-chem.* 168 (2012) 178–184.
- [35] S. Sirichai, P. Khanatharana, *Talanta* 76 (2008) 1194–1198.
- [36] Y.K. Lv, Y.N. Sun, L.M. Wang, C.L. Jia, H.W. Sun, *Anal. Met.* 3 (2011) 2557–2561.
- [37] K.C. Grabar, R.G. Freeman, M.B. Hommer, M.J. Natan, *Anal. Chem.* 67 (1995) 735–743.
- [38] X. Zhang, H. Zhao, Y. Xue, Z. Wu, Y. Zhang, Y. He, X. Li, Z. Yuan, *Biosens. Bioelectron.* 34 (2012) 112–117.